The Height of the Planetary Boundary Layer and the Production of Circulation in a Sea Breeze Model

RICHARD A. ANTHES[1]

Department of Meteorology, Naval Postgraduate School, Monterey, CA 93940

(Manuscript received 22 August 1977, in final form 7 March 1978)

ABSTRACT

A two-dimensional mesoscale model is applied to study the evolution of a strong sea breeze on a stagnant base state. In contrast to previous studies, this paper considers the relationship of the planetary boundary layer (PBL), the thermodynamic structure and the vertical circulation associated with the sea breeze in detail.

The development of the sea breeze circulation is studied quantitatively using the circulation theorem. The circulation in the vertical plane normal to the coast develops as a result of the solenoid term. The vertical diffusion of momentum acts as the most important brake on the developing circulation in agreement with previous theoretical results. The Coriolis term is small until 6 h after the heating cycle. Late in the cycle, however, it reaches a value of 45% that of the solenoid term. Horizontal and vertical advective effects are small.

Under zero geostrophic wind conditions, the return flow occurs entirely above the PBL. Therefore, neutrally buoyant pollutants emitted at the surface can only enter the return flow through the narrow zone of upward motion at the sea breeze front. Trajectories indicate that considerable recirculation toward the shore of these pollutants as well as pollutants left over in the previous day's mixed layer may occur. For the time and space scale of the sea breeze considered here, Coriolis forces are important in causing significant transports along the coast.

The depth of the circulation and the trajectories are sensitive to the rate of heating over land and the initial static stability. For strong heating in a relatively unstable environment, a significant component to the return circulation exists up to 5 km. For moderate heating in a more stable environment, there is very little return circulation above 3 km.

1. Introduction

It has been known for many years that important mesoscale circulations are produced by differential heating and cooling in the vicinity of boundaries between land and water bodies (Davis *et al.*, 1888). Important contributions to the theory of the sea breeze were made by Jeffreys (1922), Bjerknes *et al.* (1933), Godske (1934), Haurwitz (1941, 1947) and Schmidt (1947). Excellent summaries of the early observations and theories of sea breezes are given by Wexler (1946) and Defant (1951).

Although the basic structure and theory of the sea breeze was known by at least 1947 (Wexler, 1946; Schmidt, 1947), important observational studies and numerical simulations have continued to fill in the details of the sea breeze circulation and how it interacts with the planetary boundary layer (PBL) and the synoptic-scale flow. For example, Lyons (1972) and Lyons and Olsson (1973) have shown through detailed analyses of mesoscale surface, photographic, balloon, aircraft and satellite data that lake breeze circulations generated along Lake Michigan are often important in determining the trajectories of pollutants.

Much attention has been directed toward modeling the sea breeze (Estoque, 1961; Fisher, 1961; McPherson, 1970; Lambert, 1974; Walsh, 1974; Neumann and Mahrer, 1974; Pielke, 1974; Dieterle and Tingle, 1976) and much quantitative information concerning the development of the sea breeze has been derived from these studies. However, there are two aspects of the sea breeze structure that have not received much attention from a modeling point of view. These include 1) the relative importance of forces in generating and retarding the sea breeze circulation and 2) the relationship of the PBL to the onshore and offshore components of the flow. This paper considers the above problems utilizing a two-dimensional dry version of the mesoscale model described by Anthes and Warner (1978, hereafter denoted by AW).

2. Specification of the sea breeze simulation

The characteristics of the sea breeze simulation are summarized in Table 1. The grid is variable in both

[1] Permanent affiliation: The Pennsylvania State University, University Park 16802.

0022-4928/78/1231-1239$05.00

TABLE 1. Characteristics of sea breeze simulation.

$p_t = 500$ mb
$p_s = 950$ mb at $t = 0$
$\sigma = 0.0, 0.2, 0.4, 0.6, 0.68, 0.72, 0.76, 0.80, 0.84, 0.88, 0.92, 0.96, 1.0.$
$x = 0, 48, 96, 120, 144, 168, 192, 204, 216, 228, 240, 246, 252, 258, 264, 270, 276, 282, 288, 294, 300, 312, 324, 336, 348, 396, 420$ km.
$H_0 = 401.6 \sin(2\pi t/24)$ over land [W m^{-2}], $0 \leqslant t \leqslant 12$ h
$= 0$ over water
$z_0 = 0.04$ m over land
$= 0.00164$ m over water
$K_H = 2.5 \times 10^4$ m^2 s^{-1}
$\Delta t = 14$ s

the vertical and the horizontal, with highest resolution near the surface and at the coast (264 km). The vertical resolution is approximately 180 m near the ground. The heat flux is specified in this simulation according to a sine function. In Table 1, σ is the vertical coordinate defined by $(p-p_t)/(p_s-p_t)$, where p is pressure, p_t and p_s are the pressures at the top of the model and the surface, respectively, H_0 is the surface heat flux, t the time in hours, z_0 the roughness parameter and K_H the horizontal coefficient of eddy viscosity. The vertical grid is staggered with the vertical velocity $\dot{\sigma}$ defined at the σ levels listed in Table 1 and all other variables defined at the intermediate levels. The approximate elevations of these intermediate levels are shown in Fig. 3. We note that the maximum heat flux of 401.6 W m^{-2} used in the control experiment is stronger than the heat flux associated with most sea breeze situations in middle latitudes. It is more appropriate for tropical or subtropical regions.

This study utilizes a high-resolution PBL model (Busch *et al.*, 1976). The surface layer is modeled according to established similarity theory. Above the surface layer, a time-dependent eddy viscosity for heat and momentum is calculated as a function of the characteristics of the PBL, including the height of the capping inversion, the local friction velocity and the surface heat flux. The height of the PBL is defined as the first level above the ground at which the vertical gradient of potential temperature exceeds 1°C km^{-1}. Because of the coarse vertical resolution ($\sim$180 m near the ground) the model is not capable of resolving such fine-scale structures as the thermal internal boundary layer (TIBL) described by Lyons and Olsson (1973) until the depth of the feature exceeds 180 m. Furthermore, superadiabatic layers are not permitted to occur in the model in order to avoid numerical instability. Thus the PBL in this model consists of a layer next to the ground in which the potential temperature is nearly constant with height ($\partial\theta/\partial z < 1$°C km^{-1}).

The initial conditions consist of calm winds and a horizontally homogeneous temperature structure in which the average rate of potential temperature increase with height is 2°C km^{-1}. The boundary layer at this time coincides with the $\sigma = 0.96$ level ($\sim$400 m above the surface). For the sea breeze experiment, the surface pressure and temperatures at all levels are extrapolated outward on the west and east lateral boundaries. The u and v components at the boundaries remain at zero.

The vertical circulation associated with the sea breeze can be depicted by neglecting $\partial p^*/\partial t$ in the continuity equation

$$\frac{\partial p^*}{\partial t} = -\left(\frac{\partial p^* u}{\partial x} + \frac{\partial p^* \dot{\sigma}}{\partial \sigma}\right) \tag{1}$$

and calculating a streamfunction ψ according to

$$\nabla^2\psi \equiv \frac{\partial^2\psi}{\partial\sigma^2} + \frac{\partial^2\psi}{\partial x'^2} = \frac{\partial p^* u'}{\partial\sigma} - \frac{\partial p^*\dot{\sigma}}{\partial x'}, \tag{2}$$

where

$$\left.\begin{aligned} x' &= x/L \\ u' &= u/L \end{aligned}\right\} \tag{3}$$

and L is a horizontal length scale. In (1) and (2) $p^* = p_s - p_t$, u is the west–east component of velocity and $\dot{\sigma}$ is $d\sigma/dt$. Eq. (2) can be solved by relaxation given ψ on the boundary. Here we take $\sigma = 0$ and $\sigma = 1$ as the upper and lower boundaries so that these boundaries are streamlines and let L equal 348 km. At $\sigma = 1$, ψ is arbitrarily set to 0. Then ψ along the western and eastern boundaries is determined from

$$\left.\begin{aligned} \frac{\partial\psi}{\partial\sigma} &= (p^* u')_W + C \\ \frac{\partial\psi}{\partial\sigma} &= (p^* u')_E - C \end{aligned}\right\}, \tag{4}$$

where W and E refer to the west and east boundaries, respectively, and C is a small constant necessary to adjust the normal components when the mean divergence is not zero, *viz*,

$$C = -\tfrac{1}{2}\sum_{k=1}^{K} (p^* u')_W - (p^* u')_E \delta\sigma_k, \tag{5}$$

where K is the index of the lowest σ level at which velocity is defined. The neglect of the term $\partial p^*/\partial t$ is justified because it is at least an order of magnitude smaller than the two terms on the right-hand side of (1). Therefore, the maximum difference between the actual model-predicted wind u and the value of u computed from the streamfunction is less than 0.1 m s^{-1}.

3. The structure of the PBL with respect to the sea breeze circulation

Fig. 1 shows the streamfunction pattern superimposed on the isentropic cross sections at 2, 4, 6, 9

and 12 of simulation time. The height of the PBL is dotted in these figures. These depictions give a good overall view of the role of heating in producing the vertical circulation and the perturbation to the height of the mixed layer.

As the differential heating begins at 0 h, the air over land is warmed and expands in the vertical. The upward expansion of the isobaric surfaces produces an offshore acceleration of the air aloft which in turn leads to a surface pressure fall over land and concomitant onshore circulation.

The heating over land, and, to a lesser extent, the upward vertical motion there, causes a growth of the PBL. Conversely, the height of the PBL is suppressed over water by the subsidence in the absence of heating. This results in a sharp horizontal gradient in the height of the mixed layer near the coast. By 6 h, the mixed layer is about 2300 m over land compared to an average of 500 m over water. The subsidence has depressed the mixed layer height just offshore to less than 400 m.

The model's rendition of the TIBL at 6 h is shown in Fig. 1c. The heating of the marine air by the strong heat flux over land results in a rapid growth of the PBL away from the shore. The slope of the PBL is ~1:25. Because of the restriction that the PBL remain weakly stable in the mean, the isentropes in the baroclinic zone do not bend back toward the sea.

The vertical motion patterns at 6 h show a maximum upward motion of about 11 cm s^{-1} at a point 21 km inland from the coast. The maximum subsidence (also ~11 cm s^{-1}) occurs nearly on the coast.

The isentropic cross sections show the intensification of the baroclinic zone associated with the sea breeze front. At 6 h a difference of over 4°C occurs from the coast to 24 km inland.

The center of the vertical circulation occurs at 6 h just inland from the coast at a pressure of 830 mb (120 mb above the surface). The center coincides with the depth of the PBL at this point. Below the circulation center, air flows onshore across the isentropes, which is made possible by the heating. The maximum inflow of 4.8 m s^{-1} occurs 12 km inland from the coast. The air then rises in the deep, nearly isentropic PBL. It is noteworthy that the onshore component of the flow extends throughout nearly the entire depth of the PBL. The return flow, of maximum velocity 2.4 m s^{-1} at 6 h, is confined to the stable air above the PBL where the flow is isentropic. The sinking branch of the circulation, which occurs in stable air, depresses the isentropic surfaces downward which tends to reduce the baroclinity near the coast.

The characteristics of the sea-breeze simulation agree with many of the previous observational and modeling studies although some of the detailed structure may be smoothed because of the coarse resolution. The maximum onshore component of ~5 m s^{-1}, the inflow layer depth of 1 km, the maximum return flow of 2.4 m s^{-1}, and the 4 km depth of the layer of return flow are well within the range of the parameters found in observational, theoretical and modeling studies [see Wexler (1946), Schmidt (1947) and the modeling studies cited earlier]. However, the relatively coarse vertical and horizontal resolutions probably overestimate the depth of the inflow and the width of the updraft, and underestimate the intensity of the updraft associated with the sea breeze front. For example, Lyons and Olsson (1973) estimated upward velocities of over 1 m s^{-1} in a zone approximately 1 km wide in a Lake Michigan lake breeze.

The deep circulation induced in this simulation compared to some other models (e.g., Estoque, 1962; Lambert, 1974) is caused by the following three factors:

1) The strong heat flux used in this simulation. In a comparison experiment in which the heat flux was half that in this experiment, the top of the return flow (as defined by the 1 m s^{-1} isotach) was lowered from 3.9 to 2.2 km.

2) The relatively unstable sounding (lapse rate 8°C km^{-1}). Estoque (1962) utilized a lapse rate of 7°C km^{-1}, while Lambert (1974) utilized a value of 6.5°C km^{-1}. In a simulation with half the heat flux and a lapse rate of 3.5°C km^{-1}, the top of the return flow was lowered from 2.2 to 0.8 km.

3) The relatively high upper boundary utilized in this simulation (~5 km). Estoque (1962) and Lambert (1974) placed their upper boundaries at 2 km, which would tend to limit the development of the circulation in the vertical. Our results are more similar to Mahrer and Pielke's (1977) who placed their upper boundary at 6 km.

Finally, we note that the extension of the sea breeze and the associated subsidence far offshore is in agreement with observations. For example, the California sea breeze has been observed 90 km to sea at San Clemente (Wexler, 1946). It is also noteworthy that the warming of over 2°C associated with the subsidence over the water would be enough to cause the evaporation of shallow marine stratocumulus. This mechanism was proposed by Neiburger (1944) as being responsible for the diurnal minimum in the stratus off the California Coast in the afternoon. More recently, satellite observations have confirmed the strong minimum in cloudiness off the central California coast at about 1400 local time (Simon, 1977).

After 6 h, the surface heat flux begins to decrease. This decrease, together with the advection of cooler air inland from the sea, causes the baroclinic zone near the coast to weaken and to propagate inland. A similar acceleration in the afternoon was noted by Lambert (1974). At 9 h after sunrise, the circulation

center occurs ~25 km from the coast. Between 9 and 12 h the further decrease of the heat flux allows for a rapid lateral diffusion of the baroclinic zone and a movement of the circulation center to 50 km inland. The advection of cooler air inland has caused a stabilization of the PBL near the coast over land, and the height of the PBL has fallen to around 800 m here (Fig. 1e). The height of the PBL in this stage of the simulation must not be taken too literally, however, because the temperature sounding is weakly stable throughout a deep layer and the precise location of the height of the PBL depends rather critically on the mathematical definition employed in its determination.

4. The production of the sea breeze circulation

Haurwitz (1947) applied Bjerknes' circulation theorem to the sea breeze and showed that friction limits

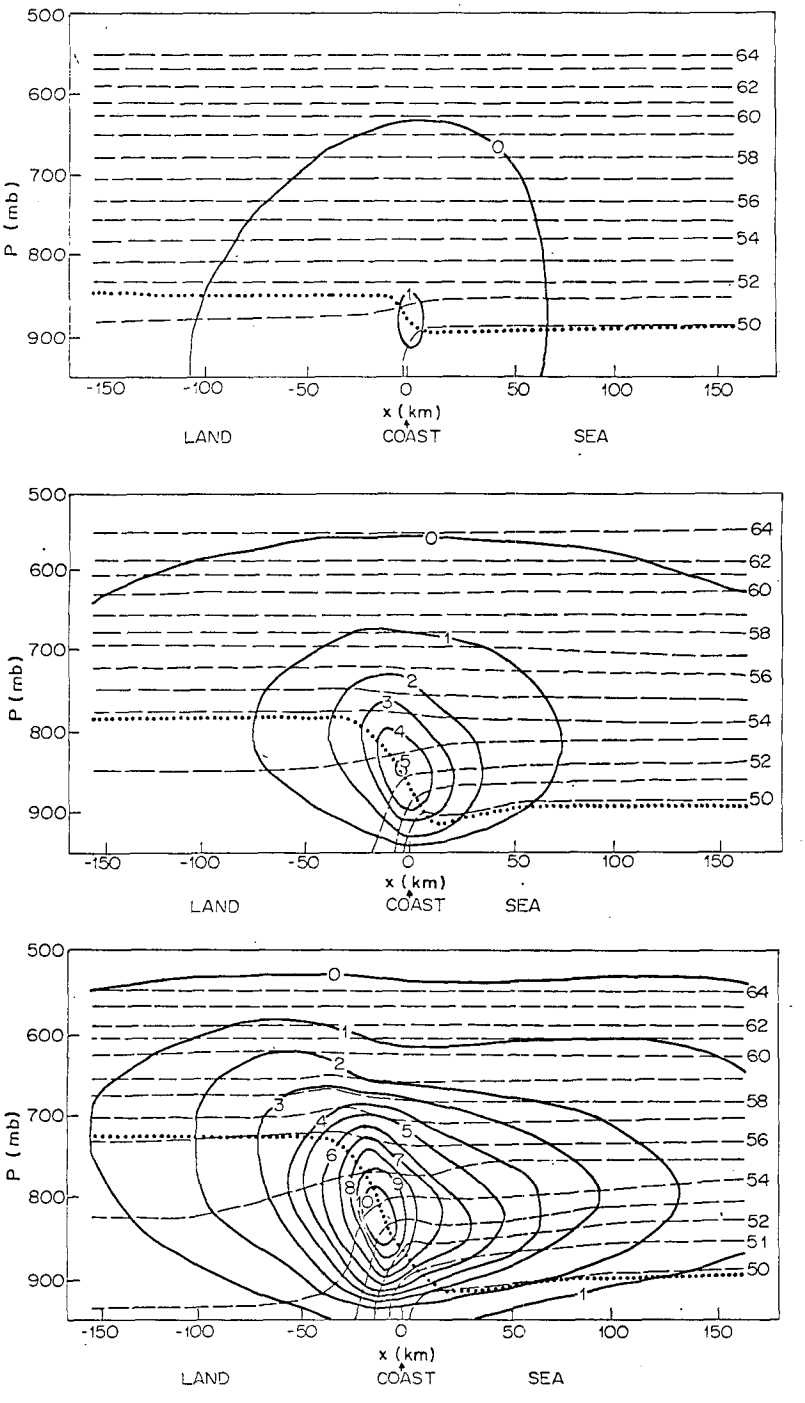

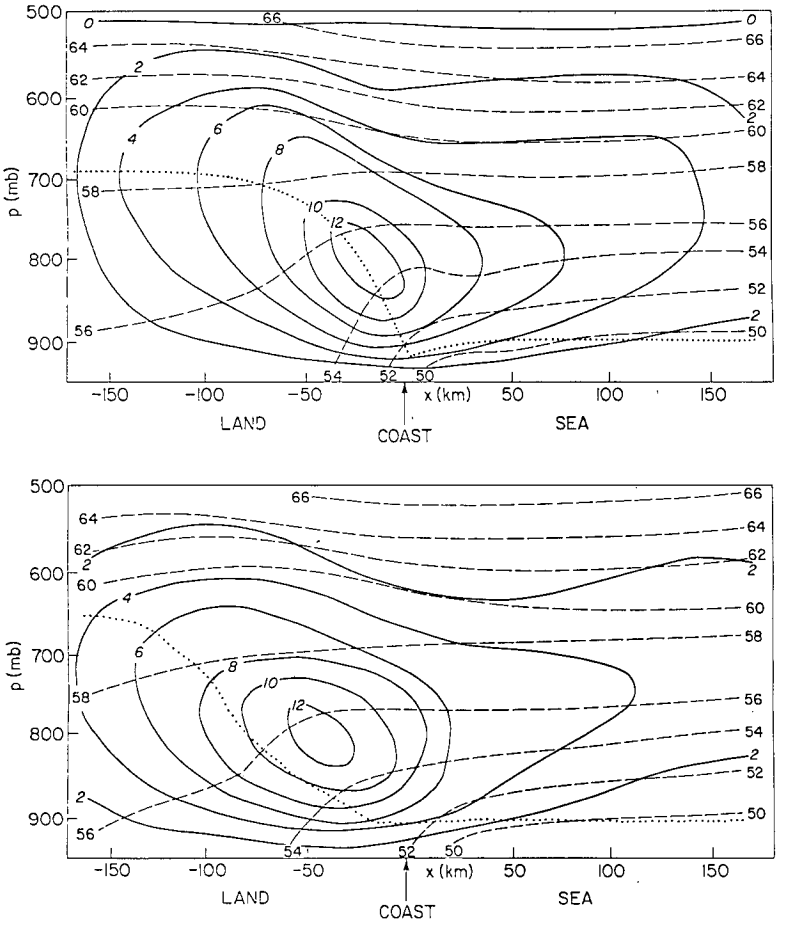

FIG. 1. Streamfunction (10^{-5} cb s^{-1}), isentropes ($\theta-250$ K) and the height of the planetary boundary layer (dotted line) at 2 h (a), 4 h (b), 6 h (c), 9 h (d) and 12 h (e).

the acceleration of the sea breeze circulation. Friction also causes the maximum temperature difference between land and sea and the wind maximum to occur at close to the same time rather than being a quarter of a period out of phase as predicted by the circulation theorem without friction. Later, Hess (1959) applied the circulation theorem to qualitatively explain the formation of the sea breeze.

The quantitative aspects of the developing sea breeze circulation can be studied by applying the circulation theorem[2] to a vertical plane perpendicular to the coast. In this way the relative contributions of the solenoid field in accelerating the circulation and the frictional forces in retarding the circulation can be ascertained. Other processes affecting the circulation are the Coriolis force and the advection of momentum. We define the circulation C around a path in the x-σ plane by

$$C=\frac{1}{\overline{p^*}}\oint \hat{\tau}\cdot p^*\mathbf{V}ds, \tag{6}$$

where $\hat{\tau}$ is the unit vector tangent to the path of integration s, which increases in a clockwise direction in the x-σ plane shown in Fig. 1, and $\overline{p^*}$ is the mean value of p^* around the path. Because the horizontal scale is typically one order of magnitude greater than the vertical scale and the horizontal motions are an order of magnitude greater than the vertical motions, we may neglect the contributions to C by vertical motions. With this approximation, the circulation is given by

$$C\approx(\overline{p^*})^{-1}\int_{x_1}^{x_2} p^*[u(x,\sigma_2)-u(x,\sigma_1)]dx. \tag{7}$$

[2] The circulation theorem here is different from that proposed by V. Bjerknes and utilized by Haurwitz (1947) and Hess (1959) in discussing the sea breeze. In their work, the circulation is studied for a closed chain of fluid particles, which is free to move about and change shape. Here, however, we consider a path fixed in space rather than following a chain of particles. Thus the nonlinear flux terms involving u and $\dot{\sigma}$ appear. This form of the circulation theorem may be considered an Eulerian form while Bjerknes' original theorem pertains to a Lagrangian coordinate system.

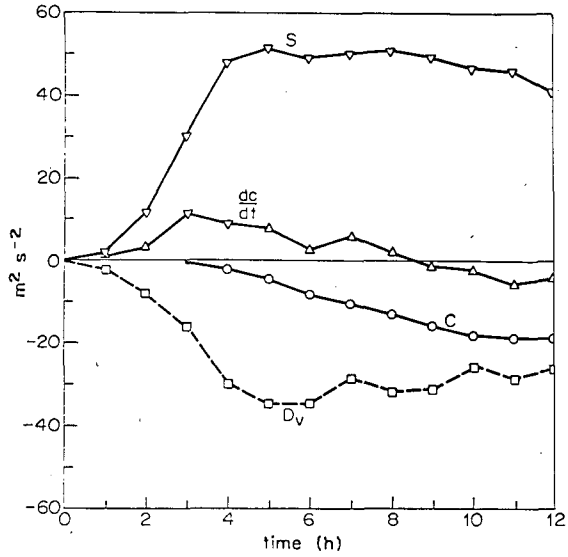

FIG. 2a. Temporal variation of the largest terms in the production of circulation: solenoid term (S), frictional force due to vertical mixing (D_V), and Coriolis force (C); also shown is rate of change of circulation due to all terms (dc/dt).

The temporal rate of change of C may be evaluated by differentiating (6) with respect to time and using the equation of motion [Eq. (24) in AW]

$$\frac{\partial C}{\partial t}=\left\{(p^*uu)_{x_1}-(p^*uu)_{x_2}+\int_{x_1}^{x_2}\left[-\frac{\partial p^*u\dot{\sigma}}{\partial\sigma}-\frac{RT}{(1+p_t/p^*\sigma)}\frac{\partial p^*}{\partial x}-p^*\frac{\partial\phi}{\partial x}+p^*fv+F_{Hu}+F_{Vu}\right]dx\right\}\Bigg|_{\sigma_1}^{\sigma_2}, \quad (8)$$

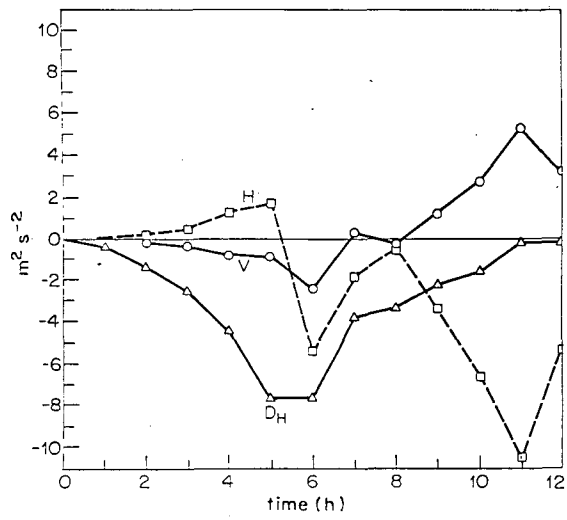

FIG. 2b. Temporal variation of smaller terms in the production of circulation: frictional force due to horizontal mixing (D_H), and accelerations due to horizontal (H) and vertical (V) fluxes of momentum.

where the σ_1, σ_2 notation means that the expression in brackets is evaluated at level σ_1 and then subtracted from the value of the same expression evaluated at σ_2. The first three terms on the right-hand side of (8) represent the production of circulation by horizontal and vertical fluxes of momentum. The fourth and fifth terms represent the acceleration by the pressure gradient force and comprise the solenoid term. The remaining terms are the Coriolis force and the horizontal (F_{Hu}) and vertical (F_{Vu}) frictional forces.

Fig. 2a shows the temporal variations of the three largest terms in the production of circulation. In this calculation, x_1 and x_2 are 12 km west and east of the coast, respectively. The vertical limits σ_1 and σ_2 are 0.98 and 0.5, which correspond approximately to pressures of 940 and 710 mb. The solenoid term grows rapidly after the heating begins, reaching a maximum of 50 $m^2 s^{-2}$ at 5 h. The vertical diffusion of momentum is the largest term opposing the solenoid term and acts as a brake on the developing circulation as proposed by Haurwitz (1947) and Schmidt (1947). The Coriolis term becomes a significant negative term after 6 h, acting to rotate the circulation into the north-south plane. The horizontal diffusion of momentum is a small negative term. The smaller terms representing the horizontal and vertical fluxes of momentum and the horizontal diffusion of momentum are shown in Fig. 2b. Only the horizontal diffusion (D_H) shows a consistent behavior over the 6 h period, acting to decrease the circulation in the x-σ plane.

The net result of all the terms, indicated by dC/dt in Fig. 2a, is positive through 8 h. At approximately 8 h, the circulation reaches its maximum intensity and the temporal rate of change of circulation becomes negative.

5. Trajectories associated with the sea breeze circulation

The strong horizontal and vertical wind shears and the rapidly changing circulation and height of the PBL complicate the transport of air pollutants in sea breeze circulations, as shown by Lyons and Olsson (1973). The nature of the Lagrangian circulations is revealed by trajectories of hypothetical air parcels (Dieterle and Tingle, 1976). Fig. 3 shows the projection onto the x-σ plane of eight 12 h trajectories of parcels originating 5 km inland from the shore at $t=0$. The elevations of the σ levels at which velocity is defined are also shown. These trajectories were computed by saving the three-dimensional velocity components every 30 min and interpolating these velocities in space and time to advect the parcels.

Fig. 3 shows that parcels of air originally above 2 km remain in the return flow during the 12 h simulation and simply get carried out to sea. The parcel originating at 1.8 km, however, subsides as it moves seaward and is eventually caught in the inflow and

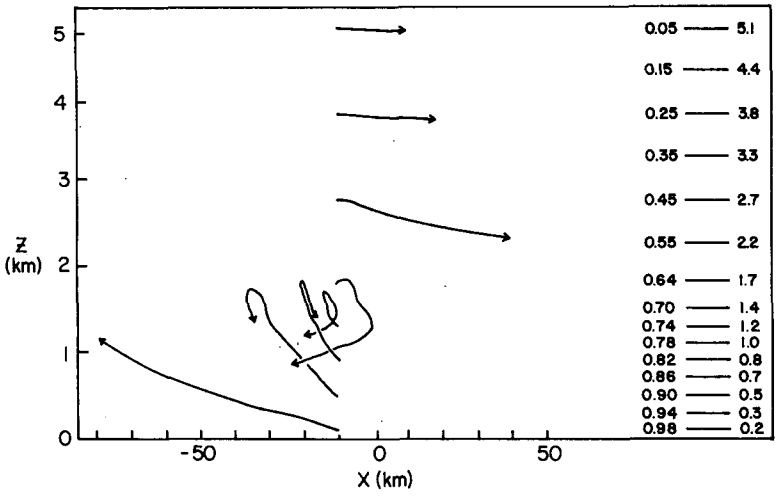

FIG. 3. Projection on the x-σ plane of 12 h trajectories associated with the control experiment. The vertical grid of the model is also illustrated.

carried back over land. The parcel at 1.2 km initially moves landward, then rises in the upward motion associated with the sea breeze front, is carried seaward in the return flow for about 3 km, subsides, and is finally caught in the inflow branch of the circulation for a second time. A similar trajectory is followed by the parcel originating at 0.9 km, but this parcel has not yet subsided back into the inflow layer at 12 h.

The parcel released at 0.5 km above the surface also is caught in the subsiding branch of the sea breeze late in the day. However, its curvature in the x-σ plane is opposite to that of the parcel released at the 0.9 km level. Finally, the parcel released closest to the ground remains in the inflow branch for the entire day. The mean vertical motions near the ground were insufficient to carry it into the return flow.

Fig. 4 shows many 12 h trajectories projected onto the x-σ plane. Air originally over water in the layer from 1–2 km subsides and is avected landward. Some of the air parcels originally over land rise in the sea breeze front and are incorporated into the return flow. Air near the surface remains in the inflow layer during the day.

Lyons and Olsson (1973) observed that pollutants released near the shore may be carried aloft in a lake breeze front and recirculate lakeward in the return flow aloft. They also note that some pollutants sink back into the inflow layer over the water. Some of the trajectories shown in Figs. 3 and 4 exhibit these characteristics. Several factors, however, make exact comparisons with Lyons and Olssons' observations impossible: 1) the heat flux used in this simulation was probably much stronger than that of the situation observed by Lyon and Olsson; 2) the initial sounding in the model was unstable compared to the observed sounding; and 3) the model's coarse horizontal resolu-

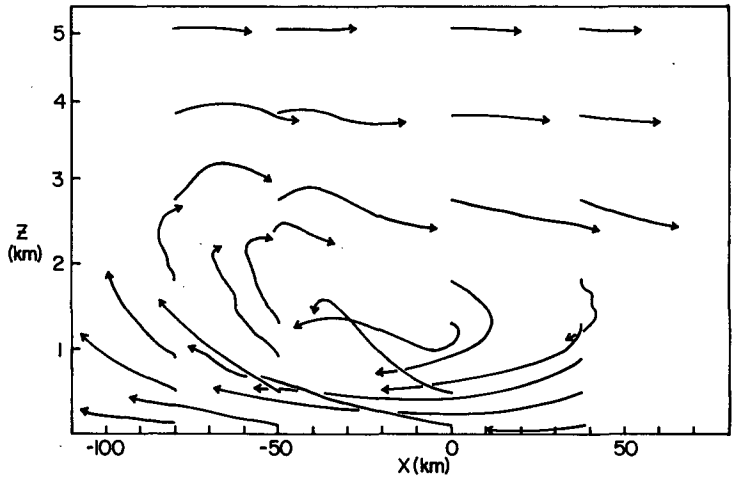

FIG. 4. Projection on the x-σ plane of 12 h trajectories associated with the control experiment.

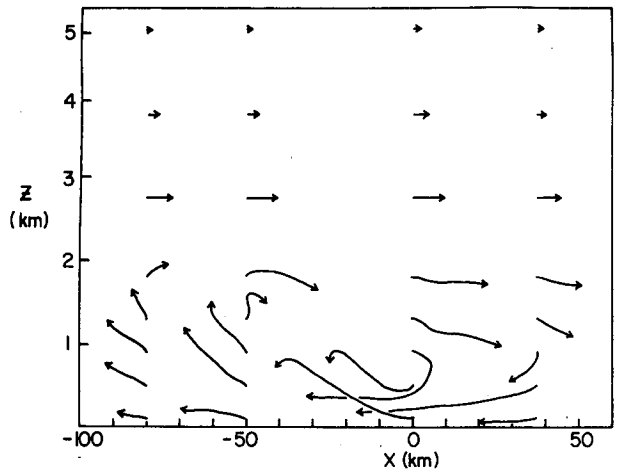

FIG. 5. As in Fig. 4 except for an experiment with half the heating rate and a more stable initial sounding.

tion almost certainly underestimates the maximum updraft by a factor of 5 or more. Thus, individual parcels that find themselves in the core of the updraft would be carried up to the level of the return flow faster than the trajectories shown in Figs. 3 and 4 indicate. Also, since the model predicts only mean vertical velocities, buoyant thermals with upward velocities more than an order of magnitude greater than the mean updraft velocities are likely present. These updrafts would make it possible for pollutants emitted at the surface to be carried rapidly up to the level of return flow, and hence complete a closed loop in less time than shown here.

In any case, the trajectories indicate that many parcels of air recirculate toward the sea, especially those above the original depth of the mixed layer. These pollutants from the deep mixed layer of the previous day are carried seaward in the return flow.

Fig. 5 shows the trajectories from an experiment designed to simulate a more shallow sea breeze. This experiment was identical to the control experiment with the exception that the heat flux was halved and the lapse rate decreased from 8 to 3.5°C km^{-1}. The mixed layer over land in this experiment grew to only 1.4 km at 6 h compared to 2.3 km of the control experiment. The trajectories shown in Fig. 5 reveal a more shallow circulation. Parcels above 3 km are displaced less than 5 km in the horizontal. The inflow layer is restricted to levels below 1.5 km. However, the general nature of the trajectories is similar to that of the control experiment.

As shown by the large magnitude of the Coriolis term in the circulation theorem, the earth's rotation significantly affects flows on these time and space scales. The result is a northward deflection of parcels moving landward (westward) in the inflow layer and a southward deflection of parcels moving seaward (eastward) in the return flow. The projections of trajectories onto the x-y plane of parcels released at 0.5 km (solid lines) and 2.7 km (dashed lines) are shown in Fig. 6. The alongshore displacements after 12 h are approximately equal to the displacements normal to the coast. A similar rightward deflection of a tetroon in the inflow layer of a lake breeze was observed by Lyons and Olsson (1973).

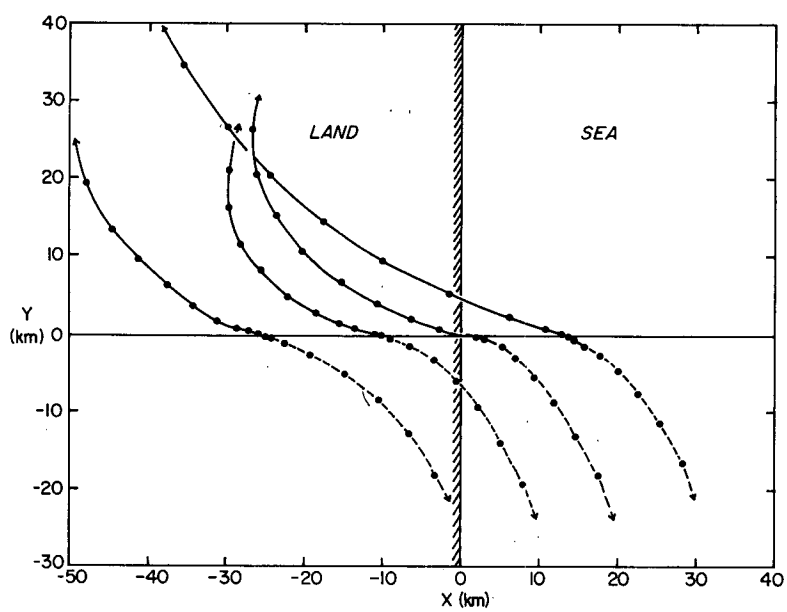

FIG. 6. Projection on the x-y plane of 12 h trajectories associated with the control experiment. Solid lines denote parcels initially at 0.5 km; dashed lines denote parcels initially at 2.7 km.

6. Summary and conclusions

A two-dimensional mesoscale model was applied to the development of a sea-breeze circulation under zero mean wind conditions. The relationship of the vertical circulation to the isentropic structure and the depth of the PBL was emphasized.

The development of the vertical circulation was investigated using the circulation theorem. During the 8 h following the beginning of the heating cycle, the solenoid term dominated the others and resulted in an increase of circulation. During the first 6 h, the greatest negative term which acted to counteract the solenoid term was the term representing vertical friction. The Coriolis force was small at the beginning, but became equal to approximately 45% of the solenoid term late in the heating cycle (10 h). The Coriolis term also opposed the solenoid term. The horizontal frictional term and the vertical and horizontal fluxes of momentum were small during the simulation. The maximum intensity of the circulation was reached around 8 h, at which time the dissipation term and the Coriolis term exceeded the solenoid term, and the circulation began to decrease..

Twelve-hour trajectories indicated the complicated paths that pollutants may take when influenced by the sea-breeze circulation. Significant recirculation toward the sea of pollutants from the mixed layer of the previous day occurs. Pollutants may also enter the return circulation from the zone of upward motion at the sea breeze front. Pollutants offshore are caught in the subsiding branch of the circulation and can be returned to the inflow layer. Finally, the Coriolis force produces an alongshore displacement comparable to the displacement normal to the coast.

Acknowledgments. Nelson Seaman assisted with the computation. Betty Bunnell and Marion Marks typed the manuscript. This work was supported by the Environmental Protection Agency through Grant R-800397 and the U.S. Army through Grant DAAG29-76-G-0157. The support of the Naval Air Systems Command during the latter portion of this study is also acknowledged. I also acknowledge the comments of the reviewers who insisted upon trajectories to show how pollutants can be recirculated seaward.

REFERENCES

Anthes, R. A., and T. T. Warner, 1978: Development of mesoscale models suitable for air pollution and other mesometeorological studies. *Mon. Wea. Rev.*, **106**, (in press).

Bjerknes, V., J. Bjerknes, H. Solberg and J. T. Bergeron, 1933: *Physikalische Hydrodynamik*. Verlag Springer, 797 pp.

Busch, N. E., S. W. Chang and R. A. Anthes, 1976: A multilevel model of the planetary boundary layer suitable for use with mesoscale dynamic models. *J. Appl. Meteor.*, **15**, 909–919.

Davis, W. M., L. C. Schultz and R. de C. Ward, 1888: An investigation of the sea breeze. *New England Meteor. Soc. Observ.*, **21**, 214–264.

Defant, F., 1951: *Compendium of Meteorology*. Amer. Meteor. Soc., 658–672.

Dieterle, D. A., and A. G. Tingle, 1976: A numerical study of mesoscale transport of air pollutants in sea-breeze circulations. *Preprints 3rd Symp. Atmospheric Turbulence Diffusion and Air Quality*, Raleigh, Amer. Meteor. Soc., 436–441.

Estoque, M. A., 1961: A theoretical investigation of the sea breeze. *Quart. J. Roy. Meteor. Soc.*, **87**, 136–146.

——, 1962: The sea breeze as a function of the prevailing synoptic situation. *J. Atmos. Sci.*, **19**, 244–250.

Fisher, E. L., 1961: A theoretical study of the sea breeze. *J. Meteor.*, **18**, 216–233.

Godske, C. L., 1934: Über Bildung und Vernichtung der Zirkulations bewegungen einer Flussigkeit. *Astrophys. Norv.*, **1**, 11–86.

Hess, S. L., 1959: *Introduction to Theoretical Meteorology*. Holt, Rinehart and Winston, 362 pp. (see pp. 244–245).

Haurwitz, B., 1941: *Dynamic Meteorology*. McGraw-Hill, 365 pp. (see pp. 139–140).

——, 1947: Comments on the sea breeze circulation. *J. Meteor.*, **4**, 1–8.

Jeffreys, H., 1922: On the dynamics of wind. *Quart. J. Roy. Meteor. Soc.*, **48**, 29–46.

Lambert, S., 1974: A high resolution numerical study of the sea-breeze front. *Atmosphere*, **12**, 97–105.

Lyons, W. A., 1972: The climatology and prediction of the Chicago lake breeze. *J. Appl. Meteor.*, **11**, 1259–1270.

——, and L. E. Olsson, 1973: Detailed mesometeorological studies of air pollution dispersion in the Chicago lake breeze. *Mon. Wea. Rev.*, **101**, 387–403.

Mahrer, Y., and R. A. Pielke, 1977: The effects of topography on sea and land breezes in a two-dimensional numerical model. *Mon. Wea. Rev.*, **105**, 1151–1162.

McPherson, R. D., 1970: A numerical study of the effect of a coastal irregularity on the sea breeze. *J. Appl. Meteor.*, **9**, 767–777.

Neiburger, M., 1944: Temperature changes during formation and dissipation of west coast stratus. *J. Meteor.*, **1**, 29–41.

Neumann, J., and Y. Mahrer, 1974: A theoretical study of the sea and land breezes of circular islands. *J. Appl. Meteor.*, **31**, 2027–2039.

Pielke, R. A., 1974: A three-dimensional numerical model of the sea breeze over south Florida. *Mon. Wea. Rev.*, **102**, 115–139.

Schmidt, F. H., 1947: An elementary theory of the land and sea-breeze circulation. *J. Meteor.*, **4**, 9–15.

Simon, R. L., 1977: The summertime stratus over the offshore waters of California. *Mon. Wea. Rev.*, **105**, 1310–1314.

Walsh, J. E., 1974: Sea breeze theory and applications. *J. Appl. Meteor.*, **31**, 2012–2026.

Wexler, R., 1946: Theory and observation of land and sea breezes. *Bull. Amer. Meteor. Soc.*, **27**, 272–287.